Journal of Applied Sciences

ISSN 1812-5654

science alert

ANSInet
an open access publisher
http://ansinet.com

Journal of Applied Sciences 11 (10): 1707-1715, 2011
ISSN 1812-5654 / DOI: 10.3923/jas.2011.1707.1715

Vibration Analysis of Flexible Gantry Crane System Subjected Swinging Motion of Payload

E. Yazid, S. Parman and K. Fuad
Department of Mechanical Engineering, Universiti Teknologi PETRONAS,
Bandar Seri Iskandar, 31750 Tronoh, Perak, Malaysia

Abstract: Vibration analysis of gantry crane system subjected to swinging motion of payload by considering the flexibility of crane framework and hoist cable is presented in this study. The equations of motion of such a system are coupled dynamic problem, where the dynamic model is obtained by modeling the dynamics of crane framework using finite element method and dynamics of a pendulum-like swinging motion of payload by Lagrange's equations. The coupled equations of motion are solved numerically using a combinational direct integration technique, namely Newmark-β and fourth-order Runge-Kutta method simultaneously. Numerical results show that the flexibility of crane framework and hoist cable has significant effect on the dynamics of gantry crane system.

Key words: Dynamic response, finite element, swinging motion, crane framework, payload

INTRODUCTION

Swinging motion is fundamental motion of variety of engineering systems which occurs in loads with vertically suspended cable. It is mostly found in crane system such as overhead cranes, gantry cranes, rotary cranes and other types of crane. An example of a crane system which is most widely used in factories, warehouse, shipping yards and nuclear facilities is gantry crane system. This crane is non-slewing-luffing crane type. In order to lift heavy payloads, gantry cranes usually have very strong structures and big dimension.

However, it is still large flexible mechanical structures and weakly damped (Rahman *et al*., 2003). This is also confirmed by Ren *et al.* (2008) that the bigger and longer crane structure, then the flexibility of the crane structure cannot be ignored anymore. The presence of elastic deformability will induce the unwanted vibration when it is subjected to dynamic loads. It may cause issues related with safety of crane system and its framework. Swinging motion of payload on flexible crane framework is coupled dynamic problem, where it constitutes nonlinear coupling terms between crane framework and payload dynamics, affecting the motion of gantry crane system.

To the author's knowledge, researches relate with swinging motion of payload on flexible structures has received little attention. Some references relate with this study can be referred in (Jerman *et al*., 2004; Oguamanam *et al*., 2001; Yang *et al*., 2007). Among those references, (Ju *et al*., 2006) has studied the swinging motion of payload in tower crane. They introduced small perturbation in solving payload dynamics for small angle of swing, rigid hoist cable and the motion of payload was restricted to pure planar and pure motion. They also concerned only in dynamic responses of crane framework.

This study is addressed to generate dynamic model of flexible gantry crane system subjected to 3D swinging motion of payload, to propose a computational technique for dynamic response prediction and to investigate the two-sided interaction between the swinging motion of payload to the dynamics of payload and crane framework. Once coupled dynamic model for the prediction of the dynamics of gantry crane system is known and then it can be used for advanced dynamic analysis, structural design and other purposes.

MATERIALS AND METHODS

Gantry crane system can be divided into two subsystems, namely gantry crane and stationary crane framework. In practice, gantry crane incorporates the interaction among trolley, hoist cable and payload under trolley and hoist mechanism. The payload is attached using hook system, hoisted from the trolley through hoist cable. For simplicity of the characteristics of the physical gantry crane, several assumptions are put forward to the proposed dynamical model. The mass of trolley and payload are modeled as lumped mass which is connected

Corresponding Author: E. Yazid, Department of Mechanical Engineering, Universiti Teknologi PETRONAS,
Bandar Seri Iskandar, 31750 Tronoh, Perak, Malaysia

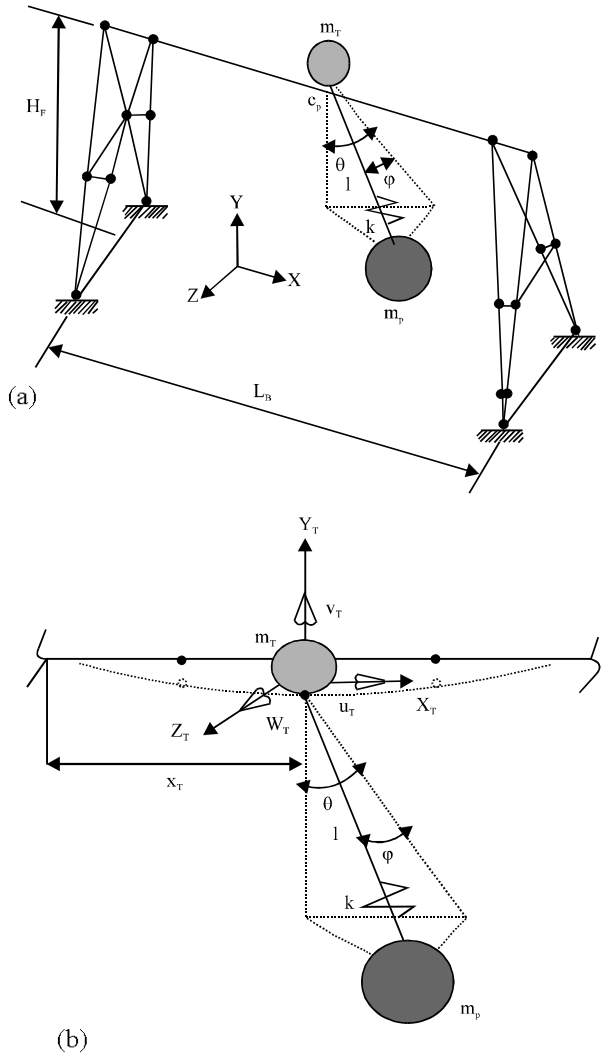

Fig 1: Model of flexible gantry crane system (a) Finite element model (b) Elastic deformation of crane framework and hoist cable

by an elastic cable. Payload and cable behave as an elastic pendulum system as shown in Fig. 1a. The payload has two swing angles with respect to the inference frame: θ is denoted as angle between the x_T-axis and x_T y_T plane, while notation φ is the angle between the cable to x_T y_T-plane as defined by Fig. 1b. The payload swings either small or large swing angles. Dynamics of hoist drive mechanism is not considered.

Dynamics of swinging motion of payload on flexible crane framework: The equations of motion of swinging motion of payload on flexible crane framework can be derived by Lagrange's equations, with the following form.

$$\frac{d}{dt}\left(\frac{\partial L}{\partial \dot{q}}\right)-\frac{\partial L}{\partial q}+\frac{\partial F}{\partial \dot{q}}=f_i, \qquad (1)$$
$$q=(u_T,v_T,w_T,\theta,\phi,\delta),\dot{q}=(\dot{u}_T,\dot{v}_T,\dot{w}_T,\dot{\theta},\dot{\phi},\dot{\delta})$$

The first three terms of $q = (u_T, v_T, w_T, \theta, \varphi, \delta)$ are defined as the generalized coordinates to describe the elastic deformations of crane framework and the rest is payload motion. General velocity of the system is denoted by q, where it is time derivative of q. The position vector of trolley r_T and payload r_P as shown in Fig. 1 can be expressed as:

$$r_T=u(x_T,t)i+v(x_T,t)j+(H_F+w(x_T,t))k \qquad (2a)$$

$$r_p=(u(x_T,t)+(\ell_p+\delta)\sin\theta\cos\phi)i$$
$$+(v(x_T,t)-(\ell_p+\delta)\cos\theta\cos\phi)j \qquad (2b)$$
$$+(H_F+w(x_T,t)-(\ell_p+\delta)\sin\phi)k$$

where i, j and k are unit vectors along the-x-, y- and z-axis, respectively. For convenience, elastic displacements in Eq. 2a and b can be expressed in following terms.

$$u_T=u(x_T,t)=u(x,t)\Big|_{x=x_T},v_T=v(x_T,t)=v(x,t)\Big|_{x=xT} \qquad (3)$$
$$w_T=w(x_T,t)=w(x,t)\Big|_{x=x_T}$$

The term x_T is position of trolley carrying a swinging payload at central point c_p of the top beam of crane framework which is time-invariant. Referring to Eq. 2, the flexibility of crane framework (u_T, v_T, w_T) and hoist cable (δ) is considered in the position vector of trolley and payload.

The flexibility of hoist cable is modeled as one linear spring with stretched length ℓ. This is sufficient approach since the cable is assumed to be in tension during normal crane operation (Masoud, 2009). The linear spring force of hoist cable can be expressed as

$$F_k=k\delta=k(\ell-\ell_p) \qquad (4)$$

It is noted that notation k is cable stiffness, while ℓ_p is unstreched hoist cable.

The Lagrangian L is defined as L = K-P, where K is kinetics energy and P is potential energy of the system. Generalized force is denoted as f_i, where they are f_x, f_y and f_z, applied input force for the x, y and z motions respectively. Kinetics energy of the system is the kinetics energy of the trolley and the payload, defined as

$$K=K_T+K_P=\tfrac{1}{2}m_T\cdot\dot{r}_T^2+\tfrac{1}{2}m_p\cdot\dot{r}_p^2 \qquad (5a)$$

The total potential energy of the system P is the potential energy of the trolley, payload and cable as follows.

$$\begin{aligned} P &= P_T + P_P + P_K \\ &= (m_T + m_p)gH_F + (m_T + m_p)gv_T \\ &\quad - m_p g(\ell_P + \delta)\cos\theta\cos\phi + \tfrac{1}{2}k\delta^2 \end{aligned} \tag{5b}$$

By deriving L with respect to generalized coordinates, then the equation motions of the system can be derived and summarized as Eq. 6a and b and the right side of Eq. 8.

$$\begin{pmatrix} -\left(\sin\theta\sin\phi/\ell_P + \delta\sin\theta\sin\phi/\ell_P^2\right)\ddot{u}_T \\ +\left(\cos\theta\sin\phi/\ell_P + \delta\cos\theta\sin\phi/\ell_P^2\right)\ddot{v}_T \\ -\left(\cos\phi/\ell_P + \delta\cos\phi/\ell_P^2\right)\ddot{w}_T + \left(1 + 2\delta/\ell_P + \delta^2/\ell_P^2\right)\ddot{\phi} \\ +2\delta\dot{\phi}/\ell_P + g\cos\theta\sin\phi/\ell_P + g\delta\cos\theta\sin\phi/\ell_P^2 \end{pmatrix} = 0 \tag{6a}$$

$$\begin{pmatrix} \sin\theta\cos\phi/\ell_P\,\ddot{u}_T - \cos\theta\cos\phi/\ell_P\,\ddot{v}_T + \sin\phi/\ell_P\,\ddot{w}_T - \dot{\phi}^2 \\ -\cos^2\phi\dot{\theta}^2 + \ddot{\delta}/\ell_P - \delta\dot{\phi}^2/\ell_P - \delta\cos^2\phi\dot{\theta}^2/\ell_P \\ -g\cos\theta\cos\phi/\ell_P + k\delta/m_P\ell_P \end{pmatrix} = 0 \tag{6b}$$

$$\begin{pmatrix} \left(\cos\theta\cos\phi/\ell_P + \delta\cos\theta\cos\phi/\ell_P^2\right)\ddot{u}_T \\ +\left(\sin\theta\cos\phi/\ell_P + \delta\sin\theta\cos\phi/\ell_P^2\right)\ddot{v}_T \\ +\left(\cos^2\phi + 2\delta\cos^2\phi/\ell_P + \delta^2\cos^2\phi/\ell_P^2\right)\ddot{\theta} \\ -\left(2\dot{\theta}\dot{\phi}\sin\phi\cos\phi\right) + 2\delta\dot{\theta}\delta\cos^2\phi/\ell_P^2 - 2\dot{\phi}\dot{\theta}\delta^2\cos\phi\sin\phi/\ell_P^2 \\ +2\delta\dot{\theta}\cos^2\phi/\ell_P + 2\delta\dot{\phi}\dot{\theta}\sin\phi\cos\phi/\ell_P + g\sin\theta\cos\phi/\ell_P \\ +g\delta\sin\theta\cos\phi/\ell_P^2 \end{pmatrix} = 0 \tag{6c}$$

Dynamics of crane framework: The crane framework model is established by the finite element method by introducing the global mass, damping and stiffness matrices of the crane framework. Based on the finite element discretization, the equation of motion for MDoF structural system, geometrically and materially linear dynamic is represented as follows:

$$[M_{st}]\{\ddot{q}_{st}(t)\} + [C_{st}]\{\dot{q}_{st}(t)\} + [K_{st}]\{q_{st}(t)\} = \{F_{st}\}(t) \tag{7}$$

where $[M_{st}]$, $[C_{st}]$, $[K_{st}]$ are the mass, damping and stiffness matrices of the crane framework, respectively; $\{\ddot{q}_{st}(t)\},\{\dot{q}_{st}(t)\},\{q_{st}(t)\}$ are the acceleration, velocity and displacement vectors for the whole crane framework respectively. Term $\{F_{st}(t)\}$ is the external forces from swinging motion of payload on the crane framework through the contact point between the trolley and the crane framework. It is assumed that swinging payload is always in contact with the top beam of crane framework.

The equations of motion for the gantry crane model associated with the generalized coordinates are combination between dynamics payload, Eqs. 6 and dynamics of crane framework, Eq. 7. It yields non-linear coupled equations of motion and written in Eq. 8.

$$\begin{aligned} &\left[[M_{st}] + \begin{bmatrix} 0 & 0 & 0 & 0 \\ 0 & (m_T + m_p) & 0 & 0 \\ 0 & 0 & (m_T + m_p) & 0 \\ 0 & 0 & 0 & (m_T + m_p) \end{bmatrix}\right] \begin{Bmatrix} \ddot{\Delta}_r \\ \ddot{u}_T \\ \ddot{v}_T \\ \ddot{w}_T \end{Bmatrix} \\ &+[C_{st}]\{\dot{q}_{st}\} + [K_{st}]\{q_{st}\} = \\ &\begin{Bmatrix} 0 \\ m_p\ell_P\begin{pmatrix} -\ddot{\theta}\cos\theta\cos\phi\left(1 + \delta/\ell_P\right) + \dot{\theta}^2\sin\theta\cos\phi\left(1 + \delta/\ell_P\right) \\ +2\dot{\theta}\dot{\phi}\cos\theta\sin\phi\left(1 + \delta/\ell_P\right) + \ddot{\phi}\sin\phi\sin\theta\left(1 + \delta/\ell_P\right) \\ +\dot{\phi}^2\cos\phi\sin\theta\left(1 + \delta/\ell_P\right) - 2\delta\dot{\theta}\cos\theta\cos\phi/\ell_P \\ +2\delta\dot{\theta}\sin\theta\sin\phi/\ell_P - \ddot{\delta}\sin\theta\cos\phi/\ell_P \end{pmatrix} \\ m_p\ell_P\begin{pmatrix} -\ddot{\theta}\sin\theta\cos\phi\left(1 + \delta/\ell_P\right) - \dot{\theta}^2\cos\theta\cos\phi\left(1 + \delta/\ell_P\right) \\ +2\dot{\theta}\dot{\phi}\sin\theta\sin\phi\left(1 + \delta/\ell_P\right) - \ddot{\phi}\cos\theta\sin\phi\left(1 + \delta/\ell_P\right) \\ -\dot{\phi}^2\cos\theta\cos\phi\left(1 + \delta/\ell_P\right) - 2\delta\dot{\theta}\sin\theta\cos\phi/\ell_P \\ -2\delta\dot{\phi}\cos\theta\sin\phi/\ell_P + \ddot{\delta}\cos\theta\cos\phi/\ell_P \end{pmatrix} \\ -(m_T + m_p)g \\ m_p\ell_P\begin{pmatrix} \ddot{\phi}\cos\phi\left(1 + \delta/\ell_P\right) - \dot{\phi}^2\sin\phi\left(1 + \delta/\ell_P\right) \\ +2\delta\dot{\phi}\cos\phi/\ell_P + \ddot{\delta}\sin\phi/\ell_P \end{pmatrix} \end{Bmatrix} \end{aligned} \tag{8}$$

Notations m_T, m_P and g are the mass of the trolley, the payload and the acceleration of gravity, respectively. Vice versa, notation $\ddot{\Delta}_r$ indicates vectors of accelerations for the rest of the degrees of freedom of the crane framework.

Numerical approach: If the swing angles, θ and φ on Eq. 6b-c and the right side of Eq. 8 are zero, the case would just be that of static load case at the central point c_P of the top beam of crane framework which imposed by $(m_t + m_p)$ load. In order to solve Eq. 6a-c and 8, the

computational scheme under Newmark-β and fourth-order Runge-Kutta method is proposed. The crane framework displacements are calculated by Newmark-β method of direct integration. The two parameters are selected as $\beta = 0.25$ and $\gamma = 0.5$, which implies a constant average acceleration with unconditional numerical stability, while payload angular displacements are calculated by Runge-Kutta method. For each integration step, Newmark-β and Runge-Kutta methods are combined simultaneously to obtain the crane framework and the payload responses.

The computational procedures with a time step of Δ_t that performs the direct numerical integration can be summarized as follows:

- Set initial condition for velocity and acceleration

$$\{q\}_0 = \{q(t=0)\}, \{\dot{q}\}_0 = \{\dot{q}(t=0)\} \quad (9)$$

- The initial external force vector $\{F\}_0 = \{F(t = 0)\}$ is calculated using right side of Eq. (8) by using initial conditions $(\theta, \dot{\theta}, \ddot{\theta}, \varphi, \dot{\varphi}, \ddot{\varphi} \text{ and } \delta, \dot{\delta}, \ddot{\delta})$ of payload

- The initial acceleration vector is calculated as

$$\{\ddot{q}\}_0 = [M_{total}]^{-1}\{\{F\}_0 - [C_{st}]\{\dot{q}\}_0 - [K_{st}]\{q\}_0\} \quad (10)$$

- Evaluation of constants from a_0 to a_7 .The parameters a_i are shown in Table 1
- The effective stiffness matrix {K} is calculated as follows

$$\{\bar{K}\} = [K_{st}] + a_0[M_{total}] + a_1[C_{st}] \quad (11)$$

- For each time step

Equations 6a-6c are solved to obtain, $(\theta, \dot{\theta}, \ddot{\theta}, \varphi, \dot{\varphi}, \ddot{\varphi} \text{ and } \delta, \dot{\delta}, \ddot{\delta})$ using fourth-order Runge-Kutta and external force vector:

Table 1: Newmark's parameters

$a_0 = \frac{1}{\beta \Delta t^2}$	$a_1 = \frac{\gamma}{\beta \Delta t}$	$a_2 = \frac{1}{\beta \Delta t}$
$a_3 = \frac{1}{2\beta} - 1$	$a_4 = \frac{\gamma}{\beta} - 1$	$a_5 = \frac{\Delta t}{2}\left(\frac{\gamma}{\beta} - 2\right)$
$a_6 = \Delta t(1-\gamma)$	$a_7 = \gamma \Delta t$	

$\{F\}_{t+\Delta t}$ is then updated. The force vector $\{F\}_{t+\Delta t}$ denotes the external loads of the system at time $t+\Delta t$.

-Equation of motion of the system is represented as below.

$$[\bar{K}]\{q\}_{t+\Delta t} = \{\bar{F}\}_{t+\Delta t} \quad (12)$$

The effective load vector {F} is below.

$$\{\bar{F}\}_{t+\Delta t} = \{F\}_{t+\Delta t} + [M_{total}]\left(a_0\{q\}_t + a_2\{\dot{q}\}_t + a_3\{\ddot{q}\}_t\right) \quad (13)$$

The displacement, velocity and acceleration responses are computed with satisfying the following relationship.

$$\{q\}_{t+\Delta t} = [\bar{K}]^{-1}\{\bar{F}\}_{t+\Delta t} \quad (14)$$

$$\{\ddot{q}\}_{t+\Delta t} = a_0\left(\{q\}_{t+\Delta t} - \{q\}_t\right) - a_2\{\dot{q}\}_t - a_3\{\ddot{q}\}_t \quad (15)$$

$$\{\dot{q}\}_{t+\Delta t} = \{\dot{q}\}_t + a_6\{\ddot{q}\}_t + a_7\{\ddot{q}\}_{t+\Delta t} \quad (16)$$

RESULTS AND DISCUSSION

The cross-sectional area of crane framework is uniform, isotropic and homogeneous material properties. The gravitational acceleration is g = 9.81 m s^{-2} and time interval is $\Delta t = 0.005$ s. Crane framework is discretized into 58 elements and 82 nodes. The issue of total number of elements and nodes will not be treated as a parameter that will be varied in the simulations. It is also noted that there is no damping either in dynamics of crane framework or dynamics of payload motion, unless particularly stated. This is expected to make it as a direct comparison with the pendulum model.

Simple case of a coupled dynamic system: The developed computer program will be verified first by solving a simple

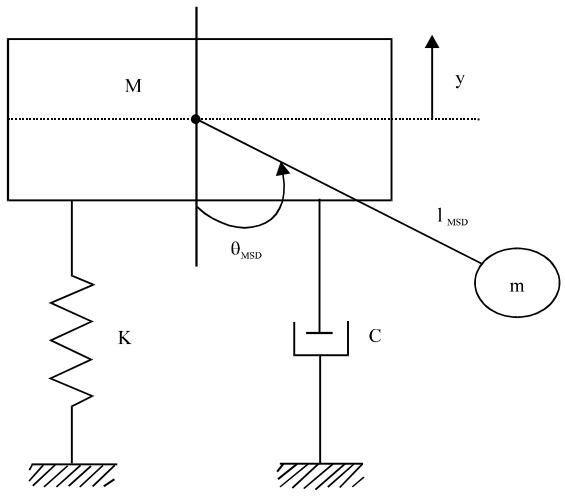

Fig. 2: Pendulum attached to a MSD system

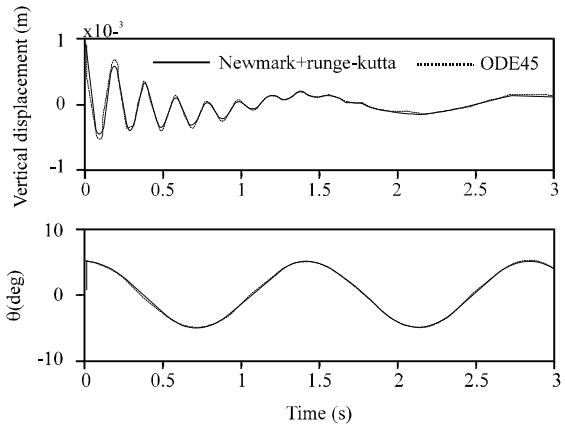

Fig. 3: Pendulum attached to a MSD displacement (a) Vertical displacements (b) Swing angle responses

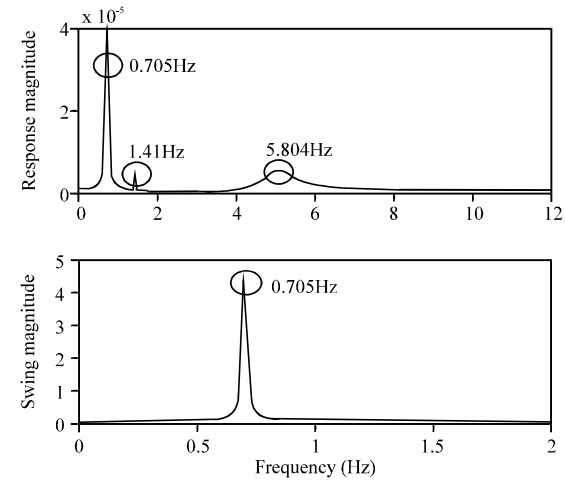

Fig. 4: FFT analysis for nonlinear model (a) Vertical response (b) Swing angle response

coupled dynamic model. The model and its equations of motion are taken from (Kyrychko *et al*., 2006), who used a simple nonlinear system consist of pendulum attached to a Mass-Spring-Damper (MSD). The configuration and the parameters of the system are depicted in Fig. 2.

Under the action of pendulum motion, the equations of motion are solved by developed Newmark-β-fourth-order Runge-Kutta and ODE-45 for nonlinear model. The displacements are shown in Fig. 3 and very good agreement between the solutions offered by both methods.

Frequency contents of vertical response in Fig. 3 are estimated using FFT analysis. There are three peak points at FFT analysis in Fig. 4, namely 0.705 Hz, 1.41 Hz and 5.804 Hz. The first peak frequency, 0.705 Hz is the natural frequency of the pendulum given by $f_p = 1/2\pi \sqrt{g/\ell_{MSD}}$

Table 2: Crane parameters

Parameters	
Trolley mass, m_T	50 kg
Payload mass, m_P	1200 kg
Cable length, ℓ_P	1 m
Stiffness cable, k	2.5e5 N m^{-1}
Initial angle, $\theta_0, \dot{\theta}_0, \ddot{\theta}_0$	5^0, 0, 0
Initial angle, $\varphi_0, \dot{\varphi}_0, \ddot{\varphi}_0$	5^0, 0, 0
Initial hoist cable displacement, $\delta_0, \dot{\delta}_0, \ddot{\delta}_0$	static,0,0

Table 3: Crane framework properties

Properties		
	Top Beam Support	Top Beam
Young's Modulus, E	2.10e11 kg m^2	
Density, ρ	7860 kg m^3	
Cross-section Area, A	3.45e-02 m^2	
		1.51e-02 m^2
Span of Framework, L_B	12 m	
Height of Framework, H_F	10.6 m	

Table 4: FFT results

	Dominant Frequency of θ (Hz)	Dominant Frequency of φ (Hz)
Rigid model	0.4985	0.4985
Flexible model	0.485	0.485

(≈ 0.705Hz) , the appearance of second frequency of pendulum 1.41 Hz. The third peak frequency, 5.804 Hz given by $f_{MSD} = 1/2\pi \sqrt{K/(M+m)}$ (≈5.804) corresponds to the natural frequencies of MSD system. It is proved that the developed computer programs are reliable and can tackle the coupled dynamic model such as MSD-pendulum system. It can be used for further study in solving coupled dynamic system in this study.

Swinging Motion of Payload on Gantry Crane System: In this subsection, swinging motion of payload and responses of crane framework are investigated as per Eq. 6a-c and 8. The parameters for cranes are shown in Table 2, while the model and the dimensions of crane framework are taken from (SPANCO, 2009) and shown in Table 3.

The dynamic responses of payload swing angles with the rigid and flexible gantry crane for time duration 20 s are illustrated in Fig. 5-6. The differences between rigid and flexible model for time window 200 s are noted with Δθ and Δφ where, $\Delta\theta = \theta_{flexible} - \theta_{rigid}$ $\Delta\varphi = \varphi_{flexible} - \varphi_{rigid}$, respectively. By observing those figures, it can be seen that flexible model has longer periods or lower frequencies than the rigid model. The deviation between the rigid assumption and the flexible model results has discernable effect.

The FFT results as shown in Table 4 reveal that swing angles frequency with flexible model is lower than that of the rigid model. This is expected since the rigid

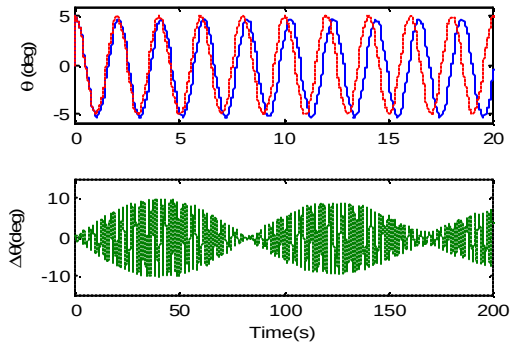

Fig. 5: Time history of swing angle (a) θ(—) flexible model, (- - -) rigid model (b) Δθ

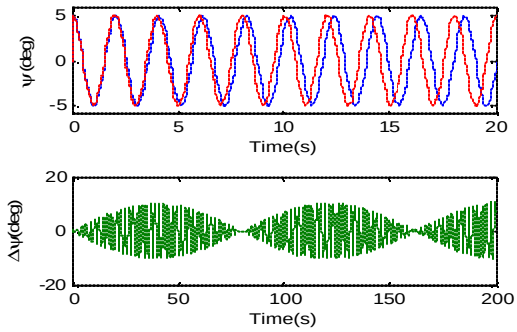

Fig. 6: Time history of swing angle (a) φ (—) flexible model, (- - -) rigid model (b) Δφ

model of crane is stiffer than the flexible crane, that's why the stiffer model vibrates at a higher frequency.

Figure 5b and 6b show a beating phenomenon either in the time histories of Δθ or Δφ. The beating phenomenon that appears in Δθ and Δφ plots because of the superimposed plot of the rigid and flexible response, which can be explained by sampling the time history of θ during 86 s, approximately 43 cycles as shown by Fig. 7a. The figure depicts that $\theta_{flexible}$ and θ_{rigid} produces a phase shift after a half cycle as shown in Fig. 7b. This phase shift accumulates over the cycles and maximum into approximately cycle 20 or 35≤t≤45s as presented by Fig. 7c. In the subsequent cycles, the accumulated phase shift decreases until approaching cycle 42 or 80≤t≤86s as shown in Fig. 7d. This behavior will repeat until prescribed time duration and so do the time history of φ.

The phase shift must be caused by the contribution of flexibility of the crane framework and hoist cable by providing acceleration in three directions to the pivot point of payload as shown in Eq. 6a-c. From those equations, it may be seen that θ couples to $\ddot{u}_T$ and $\ddot{v}_T$, φ couples with $\ddot{u}_T, \ddot{v}_T, \ddot{w}_T$ while flexibility of hoist cable in term of δ are existed in both swing angles.

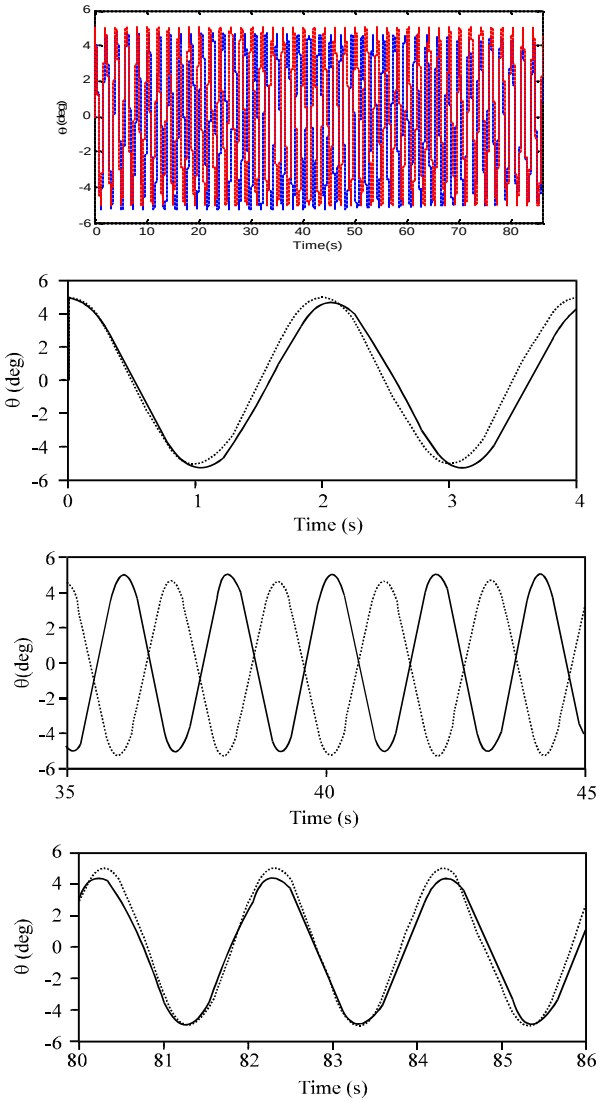

Fig. 7: Rigid and flexible model response of θ (—) flexible model, (- - -) rigid model (a) Time window0≤t≤86 s (b) 0≤t≤4 s (c) 35≤t≤45 s (d) 80≤t≤86 s

Phase portrait of $\theta_{flexible}$ and θ_{rigib} for one cycle is presented. After one cycle has been completed, the free end of $\theta_{flexible}$ noted by A' in phase portrait of Fig. 8 does not return to its original location, which is contrary with free end of θ_{rigib}, noted by B'. From those figures, it can be seen that the flexibilities significantly affect the swinging motion of payload. The effects in terms of $\ddot{u}_T, \ddot{v}_T, \ddot{w}_T$ and create difference in amplitude, frequency and phase between rigid and flexible model along the periodicity of θ and φ. It may be observed also that magnitude of swing angle for crane with flexible model is smaller than the rigid one, which is similar with work (Ren *et al.*, 2008).

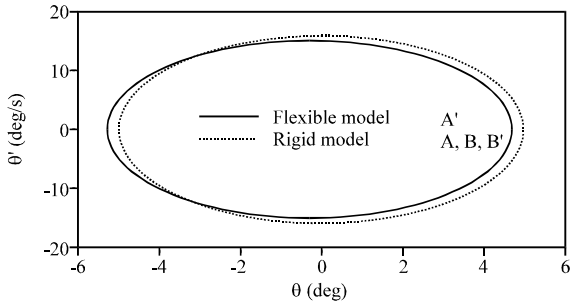

Fig. 8: Phase portrait of rigid and flexible response of θ for one cycle

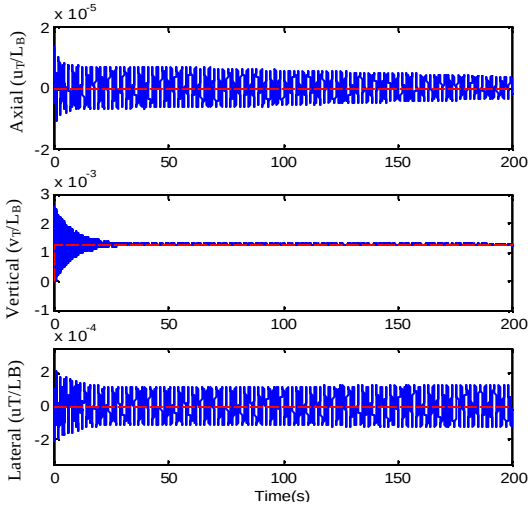

Fig. 9: Dynamic responses of crane framework (—) dynamic (….) static (a) axial (b) vertical (c) lateral displacement

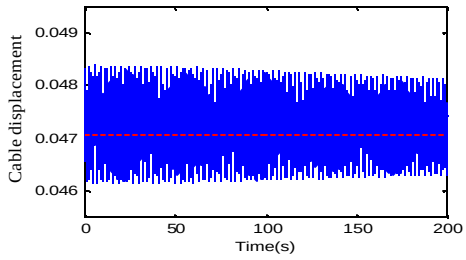

Fig. 10: Dynamic response of hoist cable (—) dynamic, (….) static

Elastic displacements of the central point c_p of top beam of crane framework are shown in Fig. 9a-c. The damping ratios are taken to be $\xi_1 = \xi_2 = 0.005$. It is seen from those figures that the structural damping significantly influences the dynamic responses of crane

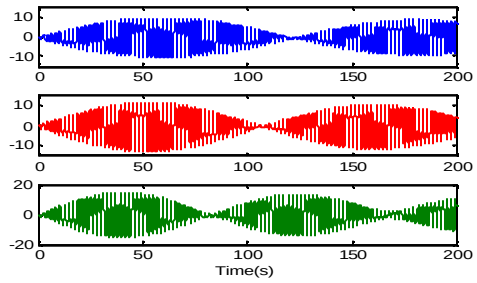

Fig. 11: Time history of Δθ (a) m_p = 700 kg (b)m_p = 900 kg C m_p = 1200 kg

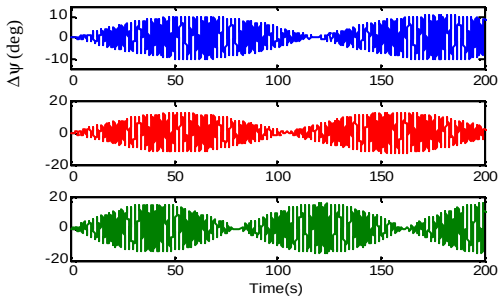

Fig. 12: Time history of Δ φ (a) m_p = 700 kg (b) m_p = 900 kg (c) m_p = 1200 kg

framework and hoist cable, particularly for the vertical (Y) displacement. At the beginning of time duration, the vibration amplitude is higher and then they vibrate as sinusoidal curve with a spatial decay about its corresponding static displacement until the end of process. Due to structural damping, the vibration converges slower and slower as time goes on. However, it will take long time to converge into its static displacement due to weakly damped (Rahman *et al*., 2003).

It is noted that the vertical axis of Fig. 9 and 10 is normalized displacements of crane framework to span length of framework top beam and hoist cable length, respectively.

Effect of payload mass variation: Except the payload mass, this simulation is conducted with parameters listed in Table 2 and 3. By means of Eq. 9, mass of payload has no effect on dynamics of payload. This is condition will be different, if the flexibility of crane framework and the hoist cable are introduced in Eq. 6a-b. The increase of payload mass has discernable effect on the payload swings, where the amplitudes and frequencies of swing angles increase with the increase of payload mass for both swing angles as shown in Fig. 11,12. This is a

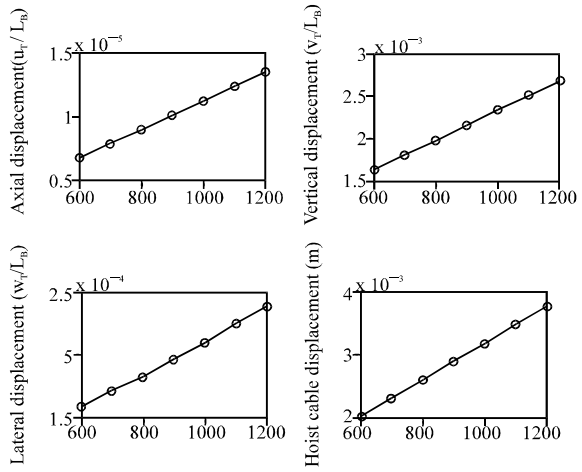

Fig. 13: Maximum dynamic responses of crane framework under payload mass variation

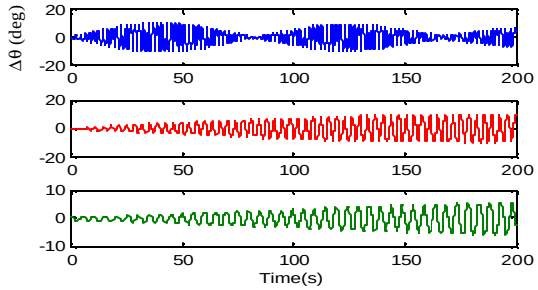

Fig. 14: Time history of Δθ (a) ℓ_p = 1m (b) ℓ_p = 3 m c ℓ_p = 6 m

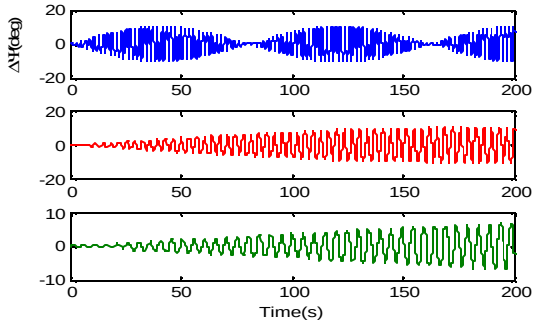

Fig. 15: Time history of Δ φ (a) ℓ_p = 1 m (b) ℓ_p = 3 m (c) ℓ_p = 6 m

reasonable result, since the displacements of crane framework and cable hoist depends on the magnitude of payload mass. The higher the payload mass, the higher

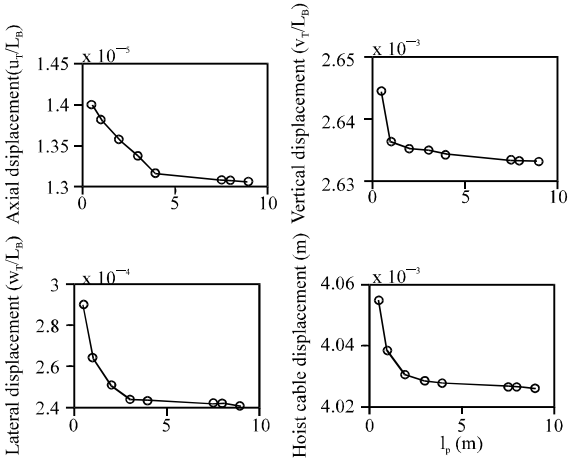

Fig. 16: Maximum dynamic responses of crane framework under cable length variation

the exciting force in the right side of Eq. 8, which in turn increasing the displacements. The larger vibration amplitudes of crane framework offer higher flexibility to pivot point of the swinging payload.

The maximum axial X, vertical Y and lateral Z displacements of the central point c_p of the top beam and cable hoist also increase with the increase of m_p as depicted in Fig.13. The increases are slightly linear for axial, vertical, lateral and hoist cable displacements.

Effect of cable length variation: Further, the cable length is varied in order to see its effect on the payload swing angles, hoist cable and crane framework. The time history results of Δθ and Δφ in Fig.14, 15 show that the amplitudes and frequencies in the payload swing responses decrease with increasing length of payload cable. The result is also found by (Oguamanam *et al.*, 2001). It may be seen that all displacements decrease with the increase of ℓ_p in Fig. 16. It can be explained by observing Fig.14-15, where the longer cable length will contributes smaller amplitudes of payload swing angles to the dynamics of crane framework. This contribution, which in turn producing smaller exciting forces for the crane framework as it can be seen in the right side of Eq. 8.

CONCLUSION

Numerical results reveal that the vibration amplitudes, frequencies and phase of the swinging payload are significantly affected by the flexibility of crane framework and hoist cable and vice versa. The flexible model of gantry crane system has longer periods or lower

frequencies compared to the rigid model. It is also found that the increase of the maximum axial X, vertical Y, lateral Z and hoist cable displacements of the central point c_p of the top beam of crane framework is slightly linear for all the displacements of crane framework under the increase of payload mass. Under the increase of cable length, the trends decrease for all the displacements.

ACKNOWLEDGMENT

The authors are thankful to Universiti Teknologi Petronas for providing the research facilities.

REFERENCES

Jerman, B., P. Podrzaj and J. Kramar, 2004. An investigation of slewing-crane dynamics during slewing motion-development and verification of a mathematical model. Int. J. Mechanical Sci., 46: 729-750.

Ju, F., Y.S. Choo and F.S. Cui, 2006. Dynamic response of a tower crane induced by the pendulum motion of the payload. Int. J. Solids Struct., 43: 376-389.

Kyrychko, Y.N., K.B. Blyuss, A. Gonzalez-Buelga, S.J. Hogan and D.J. Wagg, 2006. Real-time dynamic sub structuring in coupled oscillator-pendulum system. Proc. R. Soc. A, 462: 1271-1294.

Masoud, Z.N., 2009. Effect of hoisting cable elasticity on anti-sway controllers of quay-side container cranes. Nonlinear Dyn., 58: 129-140.

Oguamanam, D.C.D., J.S. Hansen and G.R. Heppler, 2001. Dynamics of a three-dimensional overhead crane system. J. Sound Vibrat., 242: 411-426.

Rahman, E.M.A., A.H. Nayfeh and Z.N. Masoud, 2003. Dynamic and control of crane: A review. J. Vibrat. Control, 9: 863-908.

Ren, H.L., X.L. Wang, Y.J. Hu and C.G. Li, 2008. Dynamic response analysis of a moored ship-crane with a flexible boom. J. Zhejiang Univ. Sci. A, 9: 26-31.

SPANCO, 2009. SPANCO PF series gantry crane specs. http://www.spanco.com/literature.

Yang, W., Z. Zhang and R. Shen, 2007. Modeling of system dynamics of a slewing flexible beam with moving payload swinging. Mech. Res. Commun., 34: 260-266.